Desalination and Water Treatment
www.deswater.com
1944-3994/1944-3986 © 2009 Desalination Publications. All rights reserved

9 (2009) 287–296

Vacuum membrane distillation for an integrated seawater desalination process

J.-P. Mericq, S. Laborie*, C. Cabassud

Université de Toulouse; INSA, UPS, INP; LISBP, 135 Avenue de Rangueil, F-31077 Toulouse, France
INRA, UMR792 Ingénierie des Systèmes Biologiques et des Procédés, F-31400 Toulouse, France
CNRS, UMR5504, F-31400 Toulouse, France
email: jpmericq@insa-toulouse.fr, stephanie.laborie@insa-toulouse.fr, cabassud@insa-toulouse.fr

Received 15 September 2008; Accepted 18 September 2009

ABSTRACT

Seawater desalination by reverse osmosis (RO) is widely used for drinking water production. In order to reduce the volume of brines and to increase recovery, a new approach is proposed in the frame of the European MEDINA project. It lies on a combination of RO and Vacuum Membrane Distillation (VMD) in order to over concentrated RO retentates and to reduce their volume. Indeed, VMD can be used for concentrated salty solutions, because concentration polarization and temperature polarization might be non limiting even for quite high salt concentrations. The objective of this paper is to provide some first trends on the feasibility of using VMD for enhancing the global process recovery. The approach is firstly based on simulations for highly concentrated solutions using a VMD modeling based on Knudsen diffusion through the membrane which was improved to take into account highly concentrated waters. The model was validated by experimental results obtained with different salty solutions and with both flat-sheet and hollow fiber membranes. Simulations were then performed to estimate possible performance with brines and over-concentrated sea-water in order to choose the best operating conditions for membranes of different permeability. The influence of vacuum pressure, temperature and feed water velocity was studied. As for more diluted solutions the main sensitive operating parameters are temperature and vacuum pressure. A compromise between high permeate flux obtained in these conditions and specific energetic consumption (without taking into account energy recovery) for the separation process was also discussed. Simulations showed that high permeate flux can be expected even for highly concentrated waters. With these chosen operating conditions, experiments with natural seawaters showed a permeate flux decrease with time that may be caused by some salt crystallization on the membrane, deposit of NOMs and biofouling. However, this fouling is reversible and easily removed by a hydraulic washing. These preliminary results with highly concentrated waters show the potential interest of the use of Vacuum Membrane Distillation as an integrated process with RO. Further experiments will focus on experiments with real seawaters to study more deeply fouling and biofouling phenomena for over-concentrated solutions.

Keywords: Membrane distillation; Brine disposal; Seawater desalination; High concentrations; Integrated approach

1. Introduction

On the one hand, the lack of potable water is a serious problem in many countries and the situation gets worse everyday. On the other hand, ocean and sea represent a nearly endless water resource. So, seawater desalination becomes a more attractive solution for drinking water production. Reverse Osmosis (RO) is now the main technology used for seawater desalination. However, main drawbacks of this technology are the limited recovery and the environmental impact of rejected brines. Recovery and brine concentration are limited because increasing the brine concentration in RO would increase osmotic pressure and thus the energy consumption as

---

*Corresponding author.

Presented at the Conference on Membranes in Drinking and Industrial Water Production, 20–24 October 2008, Toulouse, France.

well as scaling on the membrane surface. The European project named MEDINA (MEmbrane-based Desalination: an Integrated Approach) aimed to propose an integrated approach of desalination. One of our objectives in the frame of this project is to propose and to check the feasibility of new processes to reduce brine volumes and disposal. As a consequence, this study focuses on a combination of RO and Vacuum Membrane Distillation (VMD) in order to over concentrate RO brines and to reduce their volume (Fig. 1).

VMD is a hybrid process using both distillation and membrane process. The principle of VMD (Fig. 2) is to apply a low pressure on the permeate side of a hydrophobic micro porous membrane whereas the feed water is heated on the other side of the membrane. Water is vaporized at pore inlet and then diffuses through the membrane. At last, it is condensed outside the membrane module. The driving force of the process is the trans-membrane difference between the water vapor partial pressure at the membrane wall on the feed side and the vapor partial pressure on the permeate side. The membrane behaves as a support for the liquid/vapor interface and has no influence on the process selectivity, which depends on thermodynamics and hydrodynamics [1, 2].

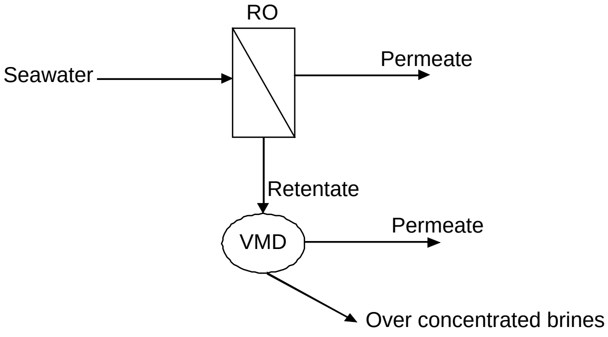

Fig. 1. RO/VMD integrated process.

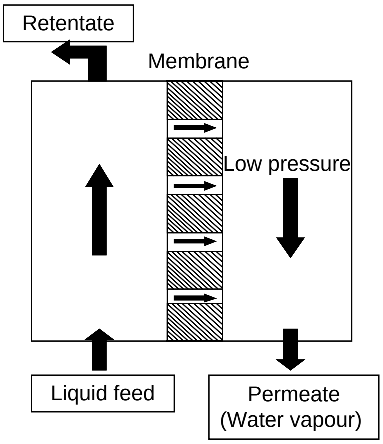

Fig. 2. VMD Principle.

VMD has already been studied for seawater desalination at "normal" salt concentration (about 35 g L^{-1}) for the direct treatment of seawater. It is now established that in this range of concentration operation at low permeate pressure and high feed temperature allows to increase the vapor permeate flux [3, 4, 5, 6]. VMD studies have shown limited concentration polarization effects for correctly chosen operating conditions and membranes, even for quite high salt concentrations [5, 6]. For the other types of membrane distillation processes, several studies focused on high concentrated sodium chloride solution and showed polarization effects [7, 8]. Some recent studies are focusing on biofouling in membrane distillation processes for seawater desalination [11].

The aim of this paper is to study the feasibility of using VMD to over concentrate RO brines and thus to be operated at very high salt concentrations from 60 g L^{-1} up to 300 g L^{-1} (concentration factor of 5). The approach is based on both experimental and computation based results.

Firstly computations have been performed considering only the salt fraction of the solution (not the DCO), without considering possible neither crystallization nor biofouling phenomena. A previously developed model [5] was improved to take into account thermodynamic properties of highly concentrated salt solutions (close to saturation). It was then validated and used for simulations with the objective to determine the range of possible maximal initial fluxes and the corresponding set of operating conditions (permeate pressure, feed temperature, hydrodynamics) and membrane characteristics. These computations aim to provide some first results on process potentiality and to discuss on more favorable operating conditions.

As this modeling cannot take into account today long term operation biofouling nor crystallization effects, because of lack of knowledge on these phenomena for VMD systems for concentrated solutions, the second step of this study aimed to perform preliminary experiments with both:

- synthetic waters (30 g L^{-1} and 300 g L^{-1}) containing only a mixture of salts representative from the Mediterranean sea to visualize time flux decline and to check if crystallization effects are limiting
- a real seawater sampled on Mediterranean sea to put in evidence possible fouling with a real sample containing both NOMs, particle, salts and susceptible to develop biofilm or scaling on the membrane.

2. Material and methods

2.1. Experimental set-up

The experiments were performed with a lab-scale pilot plant (Fig. 3) using a 0.0057 m^2 flat-sheet membrane

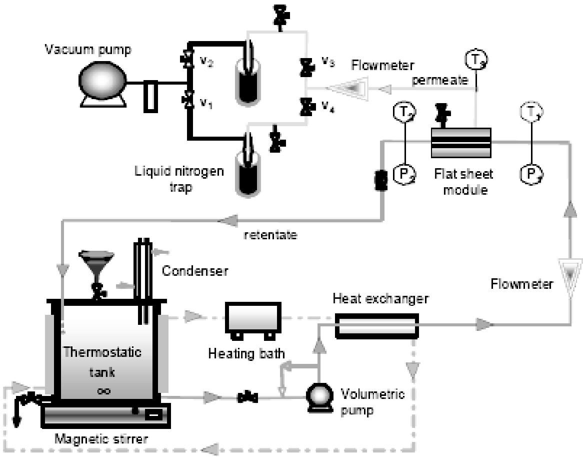

Fig. 3. Lab-scale pilot plant.

in a specific filtration module (0.21 × 0.08 m). Vacuum or low permeate pressure P_p (100–1000 Pa) was obtained using a RP 15 C Vario Vacuubrand pump. Feed water temperature T_f (298–348 K) was controlled by a thermostated tank. Liquid velocity at module inlet v ranged from 0.4 to 2.0 m s^{-1} (Reynolds Number between 850 and 7000) in the membrane module. Temperature and pressure measurements were made at module inlet and outlet and on the permeate side. At last, vapor permeate flux through the membrane was measured using a Bronkhorst thermal water mass flow meter (0 à 60 g h^{-1}). Permeate could also be collected with a cold trap made with liquid nitrogen.

Three types of feed waters were used in this study: a NaCl solution (30–300 g L^{-1}), a real Mediterranean seawater and a 300 g L^{-1} synthetic seawater solution which composition was defined in the frame of the MEDINA project and which only represents the mineral fraction of seawater. This last one was prepared by dissolving salts (composition given in Table 1 below) in pure water.

Choice of membrane properties for VMD is a key issue and it has been discussed in a previous paper [5]. Several membranes were used in this study. Three of them were non-commercial membranes M09G0020, M07R0020, M05E0020 provided by GVS Company and others were commercial membranes from Millipore (Durapore and Fluoropore) and from Desalination Systems Inc. (Desal K150). Membrane characteristics are introduced in Table 2: hydrophobicity (contact angle measures), Liquid Entry Pressure LEP (the minimal pressure for which a liquid flow through the membrane is observed) and permeability (determined using information on the vapor permeate flux measured at different transmembrane pressures).

2.2. *VMD modeling for highly concentrated salt solutions*

A VMD modeling was develop in order to simulate the VMD desalination process for both flat-sheet and hollow fiber membranes. It allows us to calculate permeate vapor flow through the membrane but also to determine concentration and temperature profiles alongside the membrane (in feed water or close to the membrane).

Table 1
Synthetic seawater composition.

Species	Na^+	K^+	Ca^{2+}	Mg^{2+}	Cl^-	HCO_3^-	Br^-	SO_4^{2-}	Total Organic Carbon
Molar percentage (%)	41.55	0.88	0.91	5.05	48.76	0.22	0.07	2.56	–
300 g L^{-1} Synthetic water (g L^{-1})	92.9	3.4	3.4	11.6	162.4	1.4	0.6	23.9	–
35 g L^{-1} Synthetic water (g L^{-1})	10.8	0.4	0.4	1.4	18.9	0.2	0.1	2.8	–
Real Seawater (g L^{-1})	11.8	0.4	0.4	1.4	21.7	0.2	0.1	3.0	1.3×10^{-3}

Table 2
Characteristics of the different membranes.

Membrane	Material	Nominal pore size (μm)	Thickness (μm)	Contact angle (°C)	LEP (10^5 Pa)	Permeability at 293.15K (s.mol$^{1/2}$ m^{-1} kg$^{-1/2}$)
M09G0020	PVDF	0.20	199	141.3	2.9	2.13×10^{-6}
M07R0020	Acrylic	0.20	202	105.8	2.9	2.56×10^{-6}
M05E0020	PTFE	0.20	218	135.1	5	3.76×10^{-6}
Durapore	PVDF	0.20	125	136.3	2.6	2.29×10^{-6}
Fluoropore	PTFE	0.22	55	123.9	4.2	3.26×10^{-6}
Desal K150	PTFE	0.10	34		> 5	1.85×10^{-5}

Its originalities are that it can represent solutions with high salt concentrations and it calculates temperature and concentration profiles at the membrane along the membrane.

It is based on a VMD modeling developed by David Wirth for hollow fiber membranes [5]. This model considers mass and heat transfer but do not consider crystallization or biofouling on the membrane. The other main assumption is to consider that vaporization occurs at pore inlet which is a support for the liquid vapor interface. Thus vaporization occurs with fluid properties corresponding to the one at the membrane temperature and concentration. Mass transfer through the membranes occurs only by diffusion of the water vapor in membrane pores. This phenomenon can be modeled by the Dusty Gas Model based on the film theory [9, 10]. It was shown that Knudsen diffusion (diffusion by collapsing between gas molecule and pore sides) mainly controls vapor transfer through the membrane if the molecules mean free path is very high compared to mean pore diameter [3, 4], which is the case in VMD when the permeate pressure is low enough. Molar water flux through the membrane J_{water} is so described by the following equation:

$$J_{\text{water}} = \left(\frac{K_M}{\sqrt{M_{\text{water}}}} (\alpha_{\text{water}} X_{\text{water}} P^*_{\text{water}}(T_m) - P_p) \right) \tag{1}$$

where X_{water}, α_{water}, M_{water} and P^*_{water} are respectively the water molar fraction, the activity coefficient, the molar mass and the vapor pressure at membrane temperature T_m; P_p is the vacuum pressure on the permeate side. Membrane Knudsen permeability coefficient K_M is related to membrane properties such as porosity (ε), thickness (δ), tortuosity (χ) and pore radius (r) but it is determined by experiments:

$$K_M = \frac{2}{3} \frac{\varepsilon . r}{\chi \delta RT} \sqrt{\frac{8RT}{\pi}} \tag{2}$$

In VMD, concentration and temperature polarization are taken into consideration only on the feed side of membrane. Following equations show respectively the concentration polarization effects (mass balance) and the temperature polarization effects (thermal balance):

$$J_{\text{water}} . M_{\text{water}} - \rho_l K_l \ln\left(\frac{\omega_{\text{salt},m}}{\omega_{\text{salt},b}} \right) = 0 \tag{3}$$

$$J_{\text{water}} . \Delta H_v - h_f (T_{fb} - T_{fm}) = 0 \tag{4}$$

where ρ_l, K_l, and h_f are respectively density, mass transfer coefficient and heat transfer coefficients of the feed seawater. $\boldsymbol{\omega}_{salt}$ and T_f are the feed total salt mass fraction and feed temperature at the membrane *m* and in the bulk *b*. ΔH_v is the molar vaporization latent heat of water. To quantify these polarizations, a concentration polarization coefficient ζ and a temperature polarization coefficient τ can be expressed as:

$$\zeta = \left(\frac{\omega_{\text{salt},b}}{\omega_{\text{salt},m}} \right) \tag{5}$$

$$\tau = \frac{T_{fm}}{T_f} \tag{6}$$

Q_{water} is the water permeate flux:

$$Q_{\text{water}} = \frac{J_{\text{water}} M_{\text{water}} * 3600}{\rho_{\text{water}}}. \tag{7}$$

Thermodynamics properties of seawater were modeled using an activity coefficient calculated by the PHREEQC software version 2.13.1 (February 15th, 2007) diffused by the US Geological Survey (USGS). This software is widely used for natural water geochemical calculation. It is an improved version of the PHRQPITZ. Mariah et al. showed that PHRQPITZ presented good correlation with experimental results for temperature between 273.15 and 333 K but could also be used up to 333K for carbonate and up to 350K for sodium chloride [7].

The set of non-linear equations (Equations 1, 2, 3) was solved using in MATLAB® the least square method as a numerical technique The main resolution is a radial numerical resolution, i.e. perpendicularly to the membrane surface. It uses the system of three nonlinear equations previously defined).

3. Results and discussion

3.1. Validation of the VMD modeling adapted to highly concentrated salt solutions

Validation of the VMD modeling was performed by comparison of experimental and computed values in the range of previously described operating conditions for the different flat-sheet membranes but also with results from works that were previously obtained at the laboratory with hollow fiber membranes for the synthetic seawater [5, 6]. Fig. 4 shows this comparison in terms of modeled flux versus experimental flux for all the different membranes and range of operating conditions. Predicted fluxes are in very good accuracy with experimental results (difference is less than 15%). VMD modeling can thus be used to predict permeate flux in order to choose the membrane and the best operating conditions.

3.2. Influence of the feed concentration

As a preliminary step, a simulation was performed to study the variation of permeate flux versus the salt molar fraction X_{salt} in the feed seawater for the Desal K150 which is the more permeable membrane. Other operating conditions were fixed to $P_p = 100$ Pa, Re = 4500 and $T_f = 313.15$ K. Fig. 5 shows these results.

As expected, in comparison with pure water, permeate flux decreases when salt concentration increases due to the variation of thermodynamic properties (activity coefficient). Fluxes obtained for the natural seawater (34 g L^{-1}, $X_{salt} = 0.009$, $Q_{water} = 47$ L h^{-1} m^{-2}) and the RO brines (60 g L^{-1}, $X_{salt} = 0.016$, $Q_{water} = 45$ L h m^{-2}) are close and much higher than the one obtained for over concentrated brines prepared with a highly concentrated synthetic seawater (300 g L^{-1}, $X_{salt} = 0.089$). However these results show that a quite high permeate flux (higher than 25 L h m^{-2}) could be obtained for the highly concentrated solution (300 g L^{-1}).

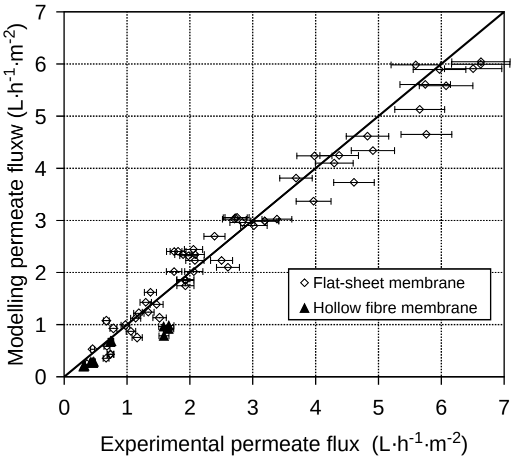

Fig. 4. Comparison between experimental and modeled permeate flux for synthetic seawater (100 Pa < *Pp* < 1000 Pa; 298 < T < 348 K; 850< Re <7000; Membranes of table 2).

3.3. Choice of an appropriate membrane

Simulations were then performed for different Knudsen Permeability of the flat-sheet membranes and for the 300 g L^{-1} synthetic seawater solution. Fig. 6 shows computed values of permeate flux for a set of chosen operating conditions which is favorable to high fluxes (low permeate pressure, turbulent flow, high temperature). Chosen conditions are $P_p = 100$ Pa, Re = 4500 and $T_f = 348$ K. As expected, higher fluxes can be reached with high Knudsen permeability membranes, for example for a very porous and thin membrane [5]. We have here to point out that long-term non-wettability of the membrane will have to be checked with real waters in further experiments to validate possible use of this membrane.

For the following simulations, two membranes were chosen that show a different permeability: Fluoropore ($K_m = 3.26 \times 10^{-6}$ s $mol^{-1/2}$ m^{-1} $kg^{-1/2}$) and Desal K150 which shows the highest permeability according to Table 2 ($K_m = 1.85 \times 10^{-5}$ s $mol^{-1/2}$ m^{-1} $kg^{-1/2}$).

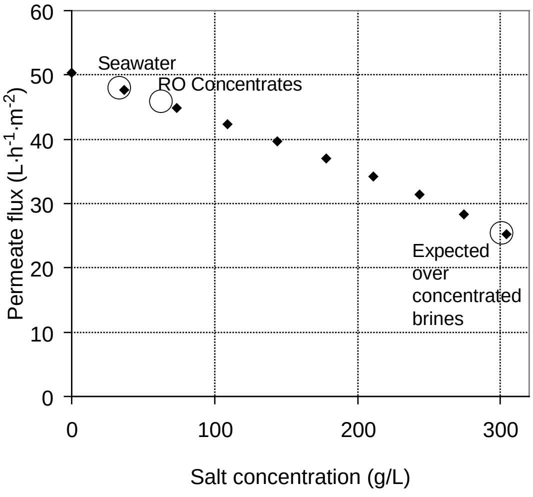

Fig. 5. Variation of permeate flux for different salt concentrations (Desal K 150, *Pp* = 100 Pa, Re = 4500 and *Tf* = 313.15 K).

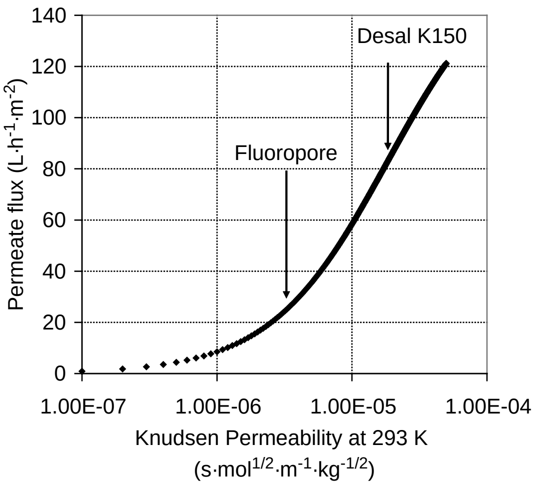

Fig. 6. Variation of VMD permeate flux with Knudsen permeability for a 300 g.L^{-1} salt solution (*Pp* = 100 Pa, Re = 4500 and *Tf* = 348 K).

3.4. Choice of the best operating conditions

With the 300 g L^{-1} synthetic seawater solution and the two chosen membranes, simulations were performed with the objective to determine the best operating conditions (feed temperature, permeate pressure and hydrodynamics) on the basis of flux and specific energy consumption criteria. For each set of experiments two operating conditions (P_p = 100 Pa, Re = 4500 and T_f = 313 K) were fixed (P_p = 100 Pa, Re = 4500 and T_f = 313 K) whereas the other one was varied. Permeate flux and the total specific energy consumption were computed. The specific energy consumption represents the quantity of energy to be provided to the membrane system per m^3 of produced water. It does not take into account the energy recovery which will occur during vapor condensation nor by energy recovery systems.

Figs. 7, 8 and 9 show results obtained respectively for a variation of permeate pressure, feed temperature and Re.

The influence of permeate pressure and of feed temperature are the same as expected and are more pronounced for the more permeable membrane (Desal K150): low pressure and high temperature allow obtaining a high permeate flux.

For given T_f and Re (Figs. 7), when P_p varies from 100 to 1500 Pa, the total energy consumption is constant and identical for the two membranes (120 kWh m^{-3}) and permeate flux is much higher (×5) for the Desal K150 and varies between 18 and 27 L h^{-1} m^{-2}. So, it will be recommended to operate at low pressure.

Feed temperature is a very sensitive operating parameter which influences significantly both flux and specific energy consumption (Fig. 8) It has a major influence on water vapor partial pressure and thus on

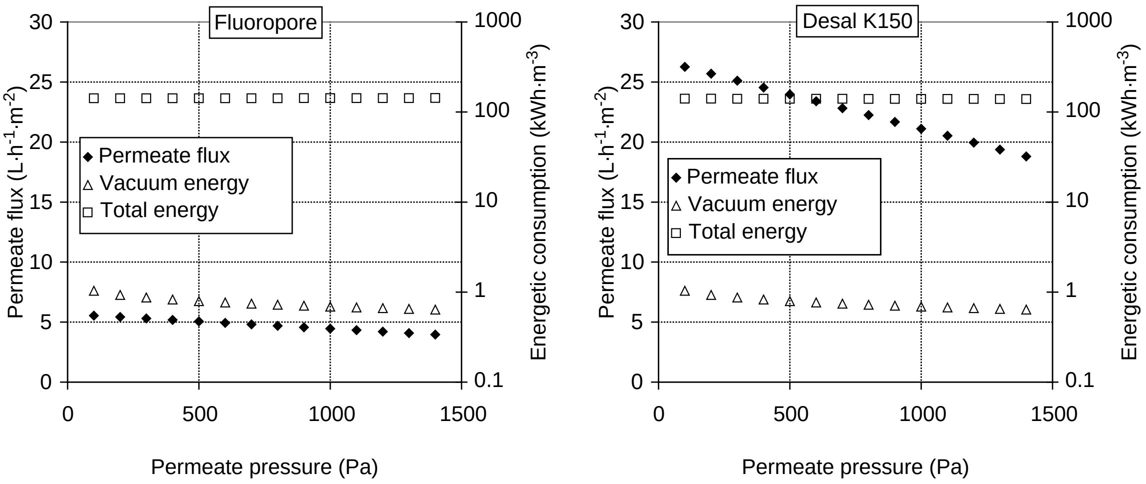

Fig. 7. Variation of permeate flux versus permeate pressure (Re = 4500, *Tf* = 313.15 K).

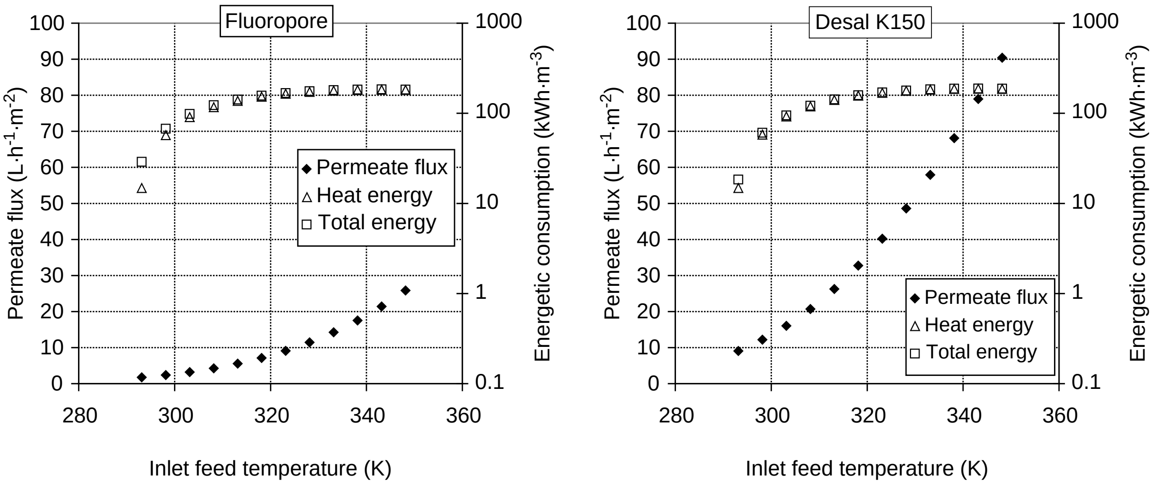

Fig. 8. Variation of permeate flux versus feed temperature (*Pp* = 100 Pa, Re = 4500).

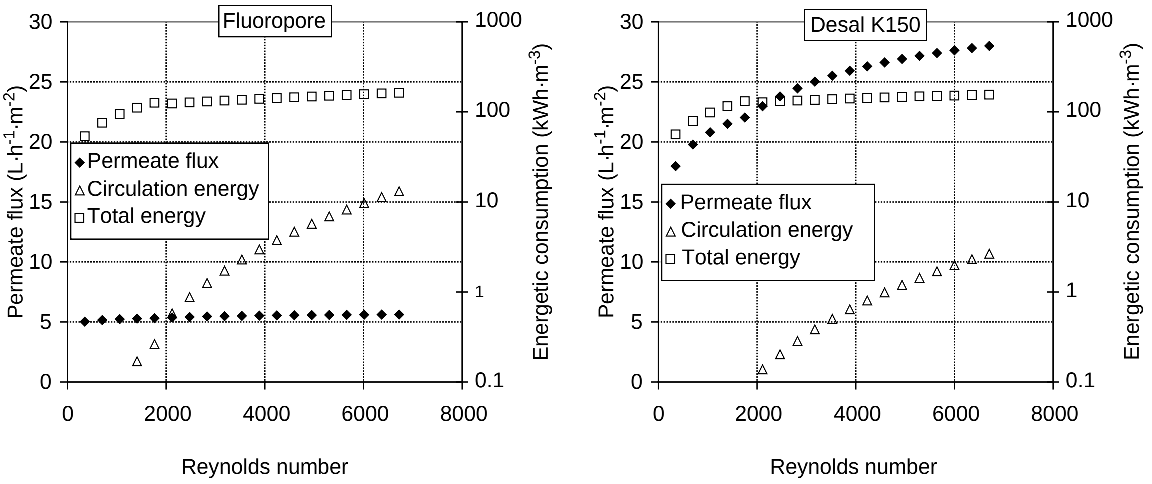

Fig. 9. Variation of permeate flux versus Reynolds number (Pp = 100 Pa, Tf = 313.15 K).

Table 3
Example of recommended operating conditions—Membrane Desal K150.

	Pp (Pa)	T*f* (K)	Re	Permeate flux (L h^{-1} m^{-2})	Circulation energy (kWh m^{-3})	Vacuum energy (kWh m^{-3})	Heat energy (kWh m^{-3})	Total required energy (kWh m^{-3})
1	100	298	4500	16	1.3	1	92	95
2	100	338	1000	37	0.004	1	122	123
3	100	338	6000	66	0.2	1	183	185

the transmembrane pressure difference, which is the driving force. Increasing feed temperature induces a higher energetic consumption. The energy to be provided to the module for heating the feed seawater represents the major energy consumption of the system (> 90 %) and it is really high. For example, it represents 183 kWh m^{-3} for a 333K temperature (Desal K150 with P_p = 100 Pa) and a 68 L h^{-1} m^{-2} permeate flux. This heat energy consumption does not take into consideration the energy recovery occurring during permeate vapor condensation.

Two solutions are thus possible to reduce this energy requirement. The first solution consists to reach the lower pressure that can be technically obtained (100 Pa for example) and to operate at low temperature (<300 K). As an example a 16.0 L h^{-1} m^{-2} permeate flux can be obtained with a 303 K temperature (Desal K 150 and P_p = 100 Pa) for a 94.6 kWh m^{-3} specific energy requirement. The other solution will be to operate with high temperature and to use a renewable energy resource (like solar energy) to heat the RO concentrate.

For the less permeable membrane, hydrodynamics has no influence on the flux (Fig. 9). This is explained by the limited temperature and concentration polarization effects which is in accuracy with results from previous works [3, 4]. For this membrane, it is more favorable to operate at low Re in laminar flow, which allows decreasing the energy requirement. However, for the more permeable membrane, higher permeate fluxes are obtained and they induce higher temperature and concentration polarization effects. Hydrodynamics has thus an important influence by limiting these polarization effects. Moreover the energy requirement increases slightly with Re in laminar flow but becomes stable in turbulent flow. As the energy requirement due to circulation is negligible in comparison with total energy, it seems preferable to operate at high Re in order to obtain the high permeate flux (28 L h^{-1} m^{-2} at Re= 6000) for a given energy requirement of 156 kWh m^{-3}, Table 3 shows some sets of interesting operating conditions for the highly permeable membranes:

For highly permeable membranes, the first solution (1) allows to obtain limited permeate flux but drastically decreases the energy requirement. The second solution (2) allows to obtain a higher permeate flux but requires a high heat energy and will be interesting if some renewable energy resources (solar thermal energy) can be used to provide this energy. Solution (3) allows increasing the flux in comparison with solution 2 but will also require an external renewable energy resource.

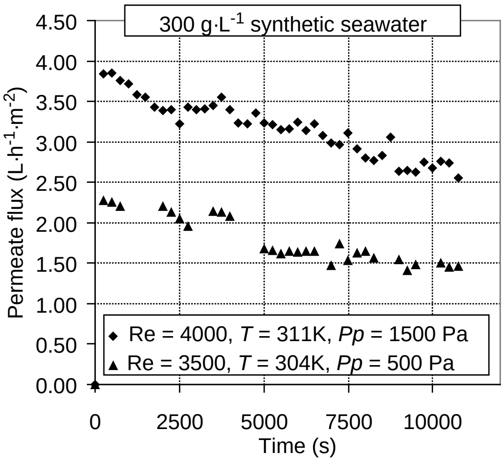

Fig. 10. Time-variation of permeate flux for 300 g L-1 synthetic seawater (Fluoropore membrane).

3.4. Experimental results with highly concentrated saline solutions

Two three-hour experiments with a 300 g L–1 synthetic seawater solution for two different operating conditions were then performed with the Fluoropore membrane. One was also performed with a 34 g L–1 real seawater. Fig. 10 below shows time-variation of the permeate flux.

For the synthetic seawater at 300 g L–1, the average permeate fluxes observed for the two sets of operating conditions are respectively 1.77 and 3.20 L h–1 m–2. These fluxes have to be compared to the initial fluxes of 2.28 and 3.84 L h–1 m–2 (2.81 and 3.31 L h–1 m–2 according to the VMD simulation). A significant flux decrease with time is observed during the experiments. Flux decrease represents 33.6 and 36.0 % respectively, in 3 h. According to computation, decrease of permeate flux is not caused by a reduction of the vapor partial pressure of the feed water, and so of the transmembrane pressure difference. Indeed, variation of the partial vapor pressure with time is negligible as temperature and concentration are nearly constant with time in the system. Simulation results show that the mean concentration and temperature polarization coefficient are respectively 0.9881 and 0.9992. Concentration at the membrane is nearly the same than in the bulk for those operating conditions, and has no influence on the process. Using feed concentration and activity coefficient at each time, a new apparent Knudsen permeability K_m was calculated at each time. This permeability shows the same decrease as the permeate flux (about 36%). Flux decline is thus explained by a modification of K_m, i.e. a modification of the membrane properties by fouling (deposit on the membrane surface or pore blocking). SEM observations of membranes after the experiments (Fig. 11) show a deposit including few salt crystals and bacteria on the membrane surface. This fouling phenomenon may explain the flux reduction. However this fouling is highly reversible and can be easily removed by a water washing. Indeed, permeability measurements before and after the experiments (after filtration and washing) show a variation of less than 5 %.

The 3-h experiment with the 34 g L–1 seawater shows a 10 % decrease of permeate flux between the beginning (4.1 L h–1 m–2) and the end (3.7 L h–1 m–2) of the experiments (Fig. 12). No apparent significant deposit was observed on the membrane surface fouling (Fig. 13). No crystals appear on the membrane surface.

Scaling was thus observed at high salt concentration for over-concentrated synthetic solutions only but not at lower concentration for real seawater when

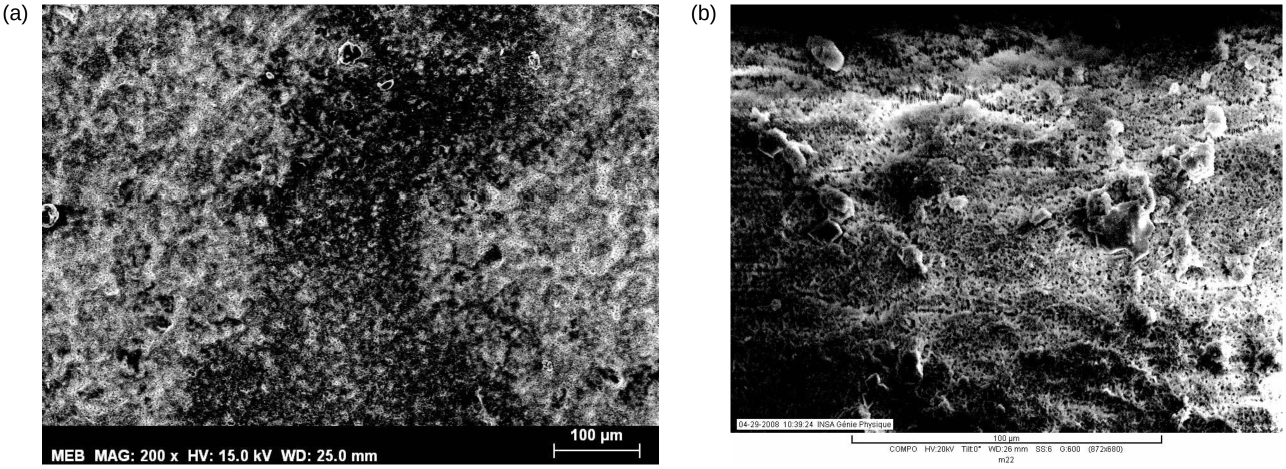

Fig. 11. Membrane surface (a) new membrane (×200) and (b) membrane after experiment (×600).

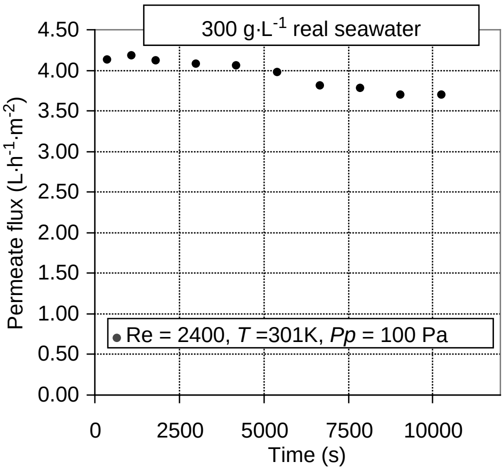

Fig. 12. Time-variation of permeate flux for real seawater (Fluoropore membrane).

organics are present in the water. Further experiments will be performed to study the combination of scaling and organic or biological fouling for highly concentrated seawaters or RO brines.

4. Conclusion

This paper aimed to study the feasibility of using VMD to over concentrate RO brines and thus to be operated at very high salt concentrations in order to reduce brine discharge volume and to increase RO global recovery factor. Studied concentrations varied from 60 g L^{-1} up to 300 g L^{-1} (concentration factor of 5). The approach was based on both experimental and computation based results.

As a first step, computations performed considering VMD of salt solutions without considering an eventual scaling or biofouling showed that, even at high salt concentration, important permeate fluxes can be reached with permeable membranes and good operating conditions. These operating conditions must be chosen in compromise between flux production and the energy requirement: a low pressure (P_p = 100 Pa), low temperatures (< 300 K) to reduce the total energy requirement and hydrodynamics conditions high enough to limit polarization effects. Indeed increasing Re allows increasing the flux whereas contribution of hydrodynamics in energy consumption is negligible. As an example, 16 L h^{-1} m^{-2} permeate flux and a 95 kWh m^{-3} energy requirement can be reached for Re = 4500 and T = 298K. Most of this energy can be recovered by permeate condensation and higher temperatures can be used if a renewable heat energy source is used.

Then experiments were performed with synthetic seawater at high salt concentration and with real seawater in order to study possible crystallization and (bio)fouling phenomena. Over periods of 3 h, no pore wetting was observed. A flux decrease with time of about 35% was observed for the highly concentrated solution but was negligible for the real seawater. The mixture of salts and dissolved organic compounds and microorganisms at seawater concentration level has no significant effect on flux or on apparent fouling. Operation at high salt concentration induces a significant fouling that is due to scaling on the membrane surface. Scaling and organic fouling are highly dependent of the feed water composition and concentration. Presence of organics can also contribute to inhibit scaling. In both cases fouling is reversible and can be easily removed by a simple water washing.

These preliminary results show the potential interest of the use of Vacuum Membrane Distillation as an integrated process with RO. Further experiments will focus on long-term experiments with RO retentates to study more deeply fouling and biofouling phenomena for over-concentrated solutions.

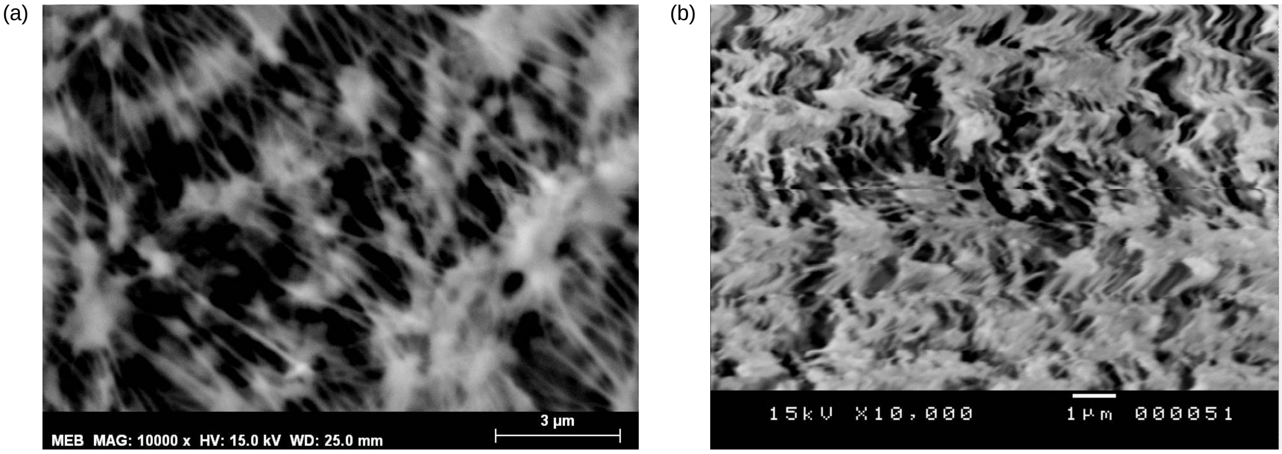

Fig. 13. Membrane surface (A) new membrane (×10 000) and (B) membrane after experiment (×10 000).

List of symbols

α_{water}	Water activity coefficient in seawater	–
χ	Membrane tortuosity	–
ε	Membrane porosity	–
δ	Membrane thickness	m
h_1	Heat transfer coefficient in feed water	$\text{W m}^{-2}\text{ K}^{-1}$
ΔH_v	Seawater molar vaporisation latent heat	J mol^{-1}
J_{water}	Water molar permeate flux	$\text{mol s}^{-1}\text{ m}^{-2}$
K_l	Mass transfer coefficient in feed water	m s^{-1}
K_M	Knudsen permeability at temperature T	$\text{s mol}^{1/2}\text{ m}^{-1}\text{ kg}^{-1/2}$
M_{water}	Water molar mass	kg mol^{-1}
P^*_{water}	Partial water vapour pressure at temperature T	Pa
Pp	Vacuum pressure on permeate side	Pa
r	Membrane pore radius	m
ρ_1	Seawater density	kg m^{-3}
ρ_{water}	Water density	kg m^{-3}
Q_{water}	Water volumic permeate flux	$\text{L h}^{-1}\text{ m}^{-2}$
T_{fb}	Temperature in feed water bulk	K
T_{fm}	Temperature on feed water side at membrane	K
T_f	Temperature in the feed water	K
τ	Temperature polarisation coefficient	–
ζ	Concentration polarisation coefficient	–
$\omega_{\text{salt},f}$	Total salt mass fraction in feed water bulk	–
$\omega_{\text{salt,m}}$	Total salt mass fraction on feed water side at membrane	–
X_{salt}	Salt molar fraction	–
X_{water}	Water molar fraction	–

Acknowledgements

This work was financially supported by the EU within MEDINA Project inside the Sixth Framework Project.

References

[1] K.W. Lawson and D. R. Lloyd. Membrane distillation. *J. Membr. Sci.*, **124**(1) (1997) 1.

[2] M.S. El-Bourawi, Z. Ding, et al.. "A framework for better understanding membrane distillation separation process." *J. Membr. Sci.*, **285**(1–2) (2006) 4.

[3] A.M. Alklaibi and N. Lior. Membrane-distillation desalination: Status and potential. *Desalination*, **171**(2) (2005) 111.

[4] Y. Xu, B.-k. Zhu, et al. Pilot test of vacuum membrane distillation for seawater desalination on a ship. *Desalination* **189**(1–3) (2006) 165.

[5] C. Cabassud and D. Wirth. Membrane distillation for water desalination: How to chose an appropriate membrane? *Desalination* **157**(1–3) (2003) 307.

[6] D. Wirth and C. Cabassud. Water desalination using membrane distillation: comparison between inside/out and outside/in permeation. *Desalination* **147**(1–3) (2002) 139.

[7] L. Mariah, C. A. Buckley, et al. Membrane distillation of concentrated brines—Role of water activities in the evaluation of driving force. *J. Membr. Sci.*, **280**(1–2) (2006) 937.

[8] Y. Yun, R. Ma, et al. Direct contact membrane distillation mechanism for high concentration NaCl solutions. *Desalination* **188**(1–3) (2006) 251.

[9] L. Martínez and F. J. Florido-Díaz. Theoretical and experimental studies on desalination using membrane distillation. *Desalination* **139**(1–3) (2001) 373.

[10] L. Martínez-Díez and M. I. Vázquez-González. Temperature and concentration polarization in membrane distillation of aqueous salt solutions. *J. Membr. Sci.*, **156**(2) (1999) 265.

[11] M. Krivorot, Y. Oren and J. Gilron. Study of factors affecting biofouling formation and biofouling in membrane distillation systems Conference on *Membrane in Drinking Water Production and Wastewater Treatment* (20–22 October 2008, Toulouse, France).